ABBI (Associative Behavior Based-Abundance Index) for Skipjack tuna (*Katsuwonus pelamis*) derived from echosounder buoys data in the Western Indian Ocean

Yannick Baidai[1], Antoine Duparc[2], Taha Imzilen [2], Amael Dupaix[2], Manuela Capello[2*]

[1] Blue Economy, Fisheries and Environmental Policy Expert, Ivory Coast.

[2] UMR MARBEC (IRD, Ifremer, Université de Montpellier, CNRS), France.

* Corresponding author : manuela.capello@ird.fr

ABSTRACT

This paper presents abundance trends for skipjack tuna (*Katsuwonus pelamis*) in the Western Indian Ocean using the Associative Behavior-Based abundance Index (ABBI). Relying acoustic data collected by echosounder buoys deployed by industrial tropical tuna purse seine fishers on drifting floating objects, the ABBI approach provides direct and effort-independent estimates of tropical tuna abundance. Compared to previous applications, the ABBI index presented in this study combines data from different echosounder buoy models, the M3I, M3I+ and M3IGO buoys (Marine Instruments inc.). The methodology which is developed allows producing a joint abundance index for skipjack tuna across buoy generations over 2013-2024.

Keywords: *Effort-independent index of abundance; Associative behavior; FADs; tropical tuna, Skipjack tuna, joint index.*

INTRODUCTION

Skipjack tuna (*Katsuwonus pelamis*) supports one of the largest tropical tuna fisheries in the Indian Ocean, with industrial purse seine fleets accounting for a substantial proportion of total catches (IOTC SC 2025). Industrial purse seine fisheries operating in the Western Indian Ocean have undergone substantial technological development over recent decades, particularly through the widespread use and continuous improvement of drifting fish aggregating devices equipped with echosounder buoys (Tidd et al. 2023). While catch-per-unit-effort (CPUE) indices are traditionally used as proxies of tuna abundance, ongoing technical changes in fishing operations and buoy technology can introduce substantial effort creep, challenging the

utilization and interpretation of CPUE time series. This highlights the need for alternative, effort-independent indices of abundance.

Recently, the Associative Behavior-Based Index (ABBI) was introduced as a direct and effort-independent indicator of tropical tuna abundance derived from echosounder buoy data. The index has been regularly evaluated within the Indian Ocean Tuna Commission (IOTC) Working Party on Tropical Tunas (WPTT) and was incorporated into the 2023 stock assessment for skipjack tuna (IOTC–WPTT25 2023). The underlying methodology was formalized in a peer-reviewed publication (Baidai et al., 2024). So far, implementations of the ABBI relied exclusively on data from a single buoy model (M3I, Marine Instruments inc.). In recent years, newer buoy generations, including M3I+ and M3iGO models from the same constructor, have progressively replaced M3I buoys in the purse seine fleet (Figure 1). To achieve consistent time series, it is necessary to incorporate the data obtained from new models into the abundance index. However, because buoy hardware and signal-processing capabilities have improved over time, differences in detection efficiency among buoy models may affect the consistency of abundance estimates and create artificial temporal trends.

This study aims to derive an ABBI index for skipjack tuna in the western Indian Ocean using data from different echosounder buoy models in order to produce a direct and effort-independent abundance indicator. First, we extend the original ABBI time series based on M3I buoys for the period 2013–2022. Second, we compute additional ABBI time series using M3I+ and M3IGO buoy models for the more recent period 2017–2024, during which these technologies became increasingly prevalent in the fishery. Finally, we construct a joint ABBI index by quantifying the relationships among M3I and M3I+ buoy signals during overlapping years (2017–2022), thereby providing harmonized abundance trends across buoy generations.

OVERVIEW OF THE ABBI INDEX

Total abundance of tropical tunas (N), calculated at a given time (t) in a given area, results from the sum of the two components of their population: the associated one (X_a), *i.e.* the tuna schools associated with floating objects, and the unassociated one, *i.e.* free-swimming schools of tunas (X_u):

$$N(t) = X_a(t) + X_u(t) \quad (1)$$

Within a given study region and time period, the average associated tuna population ($\widehat{X_a}$) can be estimated as follows:

$$\widehat{X_a} = \widehat{m}\hat{f}\hat{p} \quad (2)$$

Where $\hat{m}$ is the average tuna biomass estimated under FOBs occupied by tuna aggregation, $\hat{f}$ represents the average proportion of FOBs with tuna aggregations and $\hat{p}$ the average number of FOBs in the region of interest.

The average size of the associated component to the total population can be estimated by measuring the uninterrupted period of time that tunas spend either associated with, or disassociated from a FOB, *i.e.,* the average continuous residence time (CRT) and the average continuous absence time (CAT) (Capello et al. 2016):

$$\frac{\widehat{X_a}}{\widehat{N}} = \frac{CRT}{CRT + CAT} \quad (3)$$

Considering Equations (2-3), the total tuna population within an area can be estimated as:

$$\widehat{N} = \widehat{m}\hat{f}\hat{p}\left(1 + \frac{CAT}{CRT}\right) \quad (4)$$

Furthermore, considering Equations (1 – 2) and (4), the free-swimming population (X_u) can be expressed from the following relation:

$$\widehat{X_u} = \frac{CAT}{CRT}\widehat{m}\hat{f}\hat{p} \quad (5)$$

STUDY AREA AND PERIOD

The study area corresponds to the main fishing ground of the European purse seiners, extending over the western Indian Ocean between latitudes 10° S and 10° N and covering longitudes located between the eastern African coasts and 70° E (Figure 1). The abundance estimates were conducted in between 2013 and 2024, for each spatio-temporal strata of 10°×10° and quarter-year (Figure 2).

ESTIMATED NUMBER OF FLOATING OBJECTS ($\widehat{p}$)

The estimation of the number of floating objects (FOBs) in each of the time-area units followed two different approaches. From 2013 to 2019, it was assessed from the number of satellite-linked buoys equipping the DFADs deployed by the French tuna purse seine fleet ($n_{\text{french buoys}}$),

and two raising factors. The ratio between DFADs deployed by Spanish and French purse-seiners fleets (R_1), provided from 2010 to the end of 2017, by Katara *et al.* (2018), allowed estimates of the total number of DFADs. The missing ratios for the 2018 and 2019 were estimated using the average ratio over the year 2017, based on the assumption of a relative stabilization in the exploitation of buoys between the different fleets after this period (limitation measures on the number of buoys operated by tuna purse-seiners in the Indian Ocean: IOTC Resolutions 15/08 and 17/08). The total number of FOBs in each strata was then derived from the ratios R_2 of other floating objects (referred herein as LOGs) encountered by observers on-board French tuna seiners, consisting of natural (marine mammals, trees, etc.) or artificial (debris from human activities) floating objects found in the open ocean that are not constructed/deployed by tuna fishers, relative to the number of encountered DFADs:

$$\hat{p}_{[2013-2019]} = n_{french\ buoys}(1 + R_1)(1 + R_2) \quad (6)$$

This ratio was derived from observers' data collected through the Data Collection Framework (Reg 2017/1004 and 2016/1251) funded by both IRD and the European Union since 2005, and OCUP ("Observateur Commun Unique et Permanent"), an industry-funded program coordinated by ORTHONGEL since 2014, with an overall average coverage rate of about 50% over the years 2013 to 2017 (Goujon *et al.*, 2017). The observer data include the date, time, and location of the main activities of the vessel (e.g. fishing sets, installation or modification of FOBs, and searching for FOBs). For every activity occurring on a FOB, the type of operation (e.g. deployment, removal, and observation of a FOB) and the type of object (DFAD or LOG) are reported.

From 2020 to 2024, the estimation of FOBs number have benefited from the recent availability of buoy data from tuna purse-seine vessels provided by the IOTC Secretariat (Form 3BU). This dataset consist of the monthly mean of the number of operational buoys for each 1°×1° cell of the Indian Ocean, used as a proxy for DFAD number. DFAD number were summed over 10° cells and averaged to the quarter-year temporal resolution. FOB numbers were calculated using DFAD number and data recorded by scientific observers onboard French purse seine vessels. Using observers data, and the methodology developed in Dupaix *et al.* (2021), we calculated a mean monthly ratio (R_3):

$$R_3 = \frac{n_{LOG}}{n_{DFAD}} \quad (7)$$

with n_{LOG} and n_{DFAD} the number of LOG and DFAD observations respectively. The ratio was then used to calculated the number of FOBS per 10° cell over 2020-2024 as follows:

$$\hat{p}_{[2020-2024]} = n_{DFAD}(1 + R_3) \quad (8)$$

The total number of FOBs estimated is provided, by region and quarter, in Figure 3.

FOB-ASSOCIATED AVERAGE TUNA BIOMASS ($\hat{m}$)

The average biomasses of skipjack (size category under 10 kg) around a FOB were derived from purse seine catch-per-set data reported in the vessel logbooks of the French fleet (Table 1). FOB-associated catches-per-set reported in vessel logbooks were corrected using a dedicated procedure referred to as levels 1 and 2 of the T3 processing (Bach *et al.*, 2018; Duparc *et al.*, 2018; Depetris and Lebranchu, 2020). Level 1 adjusts the catch-per-set values declared in vessel logbooks using landing notes, to improve the accuracy of catch estimates provided by skippers. Level 2 estimates the species and size compositions of FOB sets based on port sampling data.

Since landing notes were available for all fishing trips, Level 1 was applied to correct the reported catch-per-set of all FOB sets recorded in vessel logbook data. Level 2, on the other hand, was applied only to the FOB sets conducted during the fishing trips that were sampled at landing. These FOB sets are referred to as “sampled FOB sets”.

Species compositions (i.e., percentages of catches by species and size category in the sampled FOB sets) were averaged by stratum, with a minimum threshold of 20 available sampled sets per strata. Where species composition values were missing for a given stratum, they were generated using their corresponding estimated marginal means (aka least-squares means), in a reference grid as described by Lenth (2016). The reference grid consists of the set of all combinations of predictor levels (i.e. the time-area strata) and estimated marginal means were the prediction values from the species composition models. We assessed the species composition of sets using a zero-one-inflated Beta regression model, in which the likelihood was fitted with frequentist inference (Rigby *et al.*, 2019). An equal weight of one were used for all observations, assuming representativeness in each stratum considering the sample size. The proportion of the target species in the set obtained from the sampling programs formed the response variable, while the year, quarter and spatial strata were predictors. All predictors were used to model the mean, variance, zero-inflated and one-inflated components of the model.

Model selections were performed on each model component using a Generalized Akaike Information Criterion.

The average biomasses of skipjack associated with a FOB ($\hat{m}$) were calculated for each stratum (Figure 4) by multiplying the average catch-per-set of all FOBs (including both sampled and not-sampled sets, all adjusted through the level 1 of the T3 processing) by the average species composition. Only the strata with at least 20 FOB sets (including both sampled and not-sampled sets) were considered.

PROPORTION OF INHABITED FOBS ($\hat{f}$)

Acoustic data collected by the Marine Instruments echosounder buoys were translated into presence/absence of a tuna aggregation, using a machine learning algorithm based on a random forest approach trained on logbook and observer data (Baidai et al., 2020). Because buoy technology has evolved substantially over time, both in terms of hardware and signal-processing software, each buoy model was analysed separately to account for potential differences in detection performance and sensitivity (Diallo et al. 2019).

The first sections of presence or absence occurring at the beginning of the FAD trajectories were excluded from the analysis as they may result from the colonization period of the DFAD or potentially from classification errors related to the operation on the buoy (Baidai *et al.,* 2020).

For each buoy model, daily presence/absence data were then used to derive the proportion of FOBs inhabited by a tuna aggregation (f). This was expressed as the number of DFADs (equipped by an M3I, M3I+ buoy model, respectively) classified as inhabited by a tuna aggregation, divided by the total number of buoys of the same model at a daily scale. A threshold of at least 10 available buoys per day and space-time unit was considered for the calculation of the daily proportion of inhabited FOBs. Quarterly averages of the proportion of inhabited FOBs were then calculated. Because an accurate species discrimination from these acoustic data was not possible, these values were corrected with the occurrence of skipjack tuna in the FOB-associated tuna aggregations, according to Equation (6):

$$f(SKJ) = f\eta(SKJ) \quad (9)$$

where $\eta(SKJ)$ represents the ratio between the number of FOB-associated catches with a biomass of skipjack tuna relative to the total number of positive FOB catches (considering only FOB-associated catches with a total biomass greater than or equal to 1 tonne). This ratio was estimated on a quarterly basis, within each grid cell, using the sampling data raised to the catch

per set. A minimum number of 20 available sampling data per strata was considered for the ratio calculation. Missing occurrence values for a given stratum were estimated from a binomial model using year, quarter and spatial strata as predictors. The fraction of occupied FOBs by tuna aggregations obtained for each buoy model is shown in Figure 5.

CONTINUOUS RESIDENCE TIME OF SKIPJACK TUNA (CRT)

Tuna CRTs have been shown to vary according to their species, size (Ohta et Kakuma, 2005; Robert *et al.*, 2012, Rodriguez et al. 2017) and FOB density (Pérez *et al.*, 2020). Nevertheless, numerous studies across all tropical oceans have shown that the magnitude of these variations remains relatively small for the three tuna species and the life stages considered in this work (Dagorn *et al.*, 2007; Matsumoto *et al.*, 2014, 2016; Tolotti *et al.*, 2020; Govinden *et al.*, 2021). Considering this characteristic, a constant CRT value was assumed for skipjack tuna in all spatial and temporal strata. The value was provided by Govinden et *al.* (2021), who measured an average CRT at DFADs for skipjack tunas of 4.58 ± 4.78 days.

CONTINUOUS ABSENCE TIME OF SKIPJACK TUNA (CAT)

At the time of the study, only CRTs were measured for the three species on DFADs. However, acoustic tagging experiments conducted in arrays of anchored Fish Aggregating Devices (AFADs) showed that CATs decrease for decreasing distances among AFADs, due to an increased AFAD encounter rate by tuna at higher AFAD densities (Pérez *et al.*, 2020). Based on these findings, the following Ansatz relating the average CAT to the number of FOBs ($\hat{p}$) was used:

$$CAT = \frac{1}{\phi \hat{p}} \tag{10}$$

where ϕ is a parameter that depends on the probability of associating to one of the estimated $\hat{p}$ FOBs. To assess the sensitivity of the ABBI to ϕ values, a range of 2e-05 and 6e-05 that produces CAT values that produces average CATs ranging between 10 and 30 days, consistent with the findings from acoustic tagging studies (Robert *et al.*, 2013; Rodriguez-Tress *et al.*, 2017; Pérez *et al.*, 2020) and total catches in the study area, was considered.

JOINT ABBI INDEX OF ABUNDANCE COMBINING DIFFERENT BUOY MODELS

Because successive generations of buoys differ in both hardware and onboard processing, variations in sensitivity in detecting tuna aggregations presence/absence can be observed (Diallo et al., 2019). As a result, the construction of the abundance time series required additional standardisation to ensure consistency and comparability across years and buoy generations.

First, a linear model was applied to estimate the correlation of the fraction of occupied FADs obtained for the M3+ model as response variable, and corresponding indices obtained from M3I as covariate (Figure 6, Table 2):

$$f_{M3+,i,q} = LM(f_{M3I,i,q})$$

Where $f_{M3+,i,q}$ corresponds to the fraction of occupied M3+ buoys in a 10° cell i and quarter q stratum, $f_{M3I,i,q}$ denotes the same quantity obtained using buoy model M3I estimated over the same stratum.

Then the value of $f_{M3I,i,q}$ was corrected according to the fitted model, relying on the fact that M3I+ provided a higher capability in detecting small aggregations (Diallo et al. 2019). Because M3IGO provided results consistent with M3I+ (Figure 5), no correction was applied on M3IGO. Abundance estimates were conducted for each buoy model considering a spatio-temporal stratification of 10°/ quarter. In each 10°×10° grid cell, the associated, free-swimming and total skipjack abundance was calculated following respectively the Equations (2), (5) and (4). An average quarterly index was then estimated for the whole study area for each buoy model, considering the average over the spatial strata with available data for the same period. The relative joint ABBI index (Figure 7) was calculated as the weighted mean of the ABBI indices for each buoy model and each value of ϕ (see Eq. 10), using the number of buoys of each model as weights. The first quarter of 2013 was used as the reference period. The resulting index was then averaged across all values of ϕ (Figure 8).

FIGURES AND TABLES

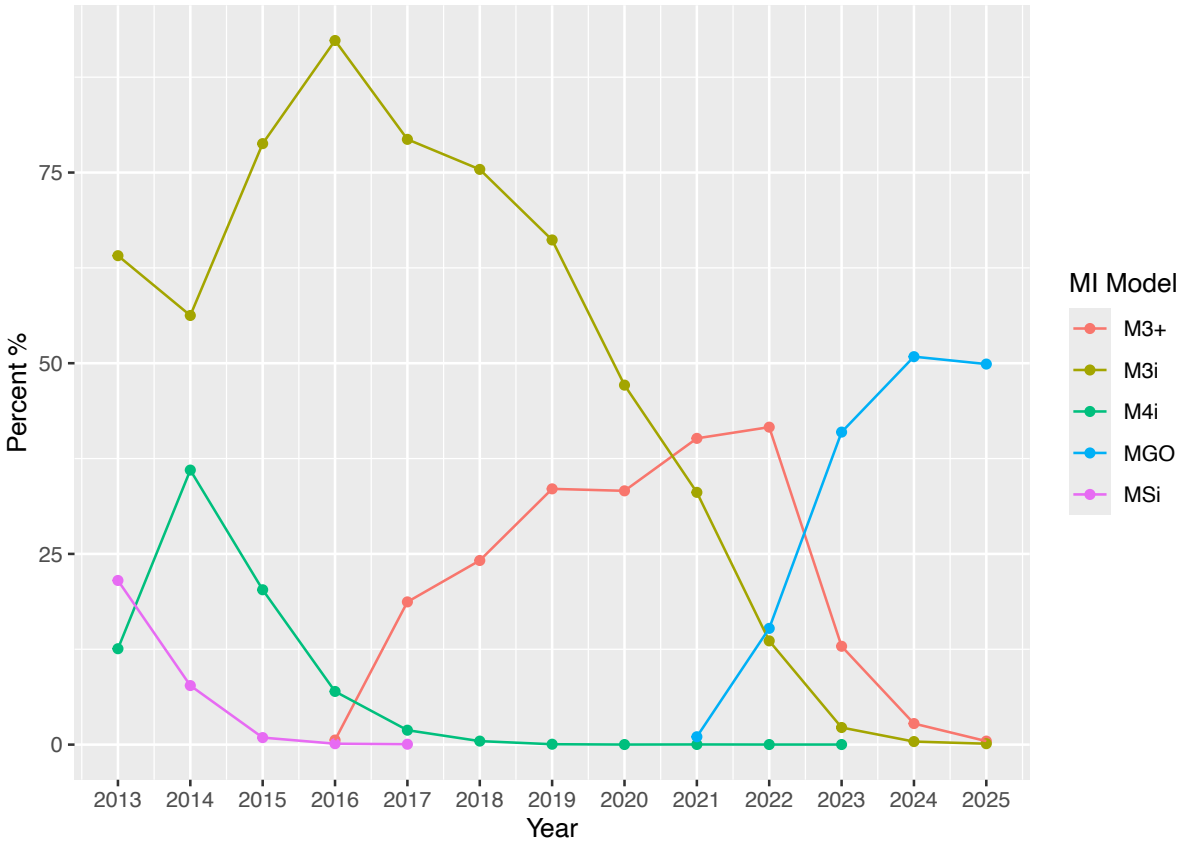

Figure 1: Percentage of Marine Instruments buoys for each model available in the Ob7 buoys database (data provided by the French fleet) in the Indian Ocean. Buoy models are identified using the three-character abbreviations provided by the manufacturer and appearing in the raw acoustic files: M3I+ is hereafter referred to as M3+, M3iGO as MGO.

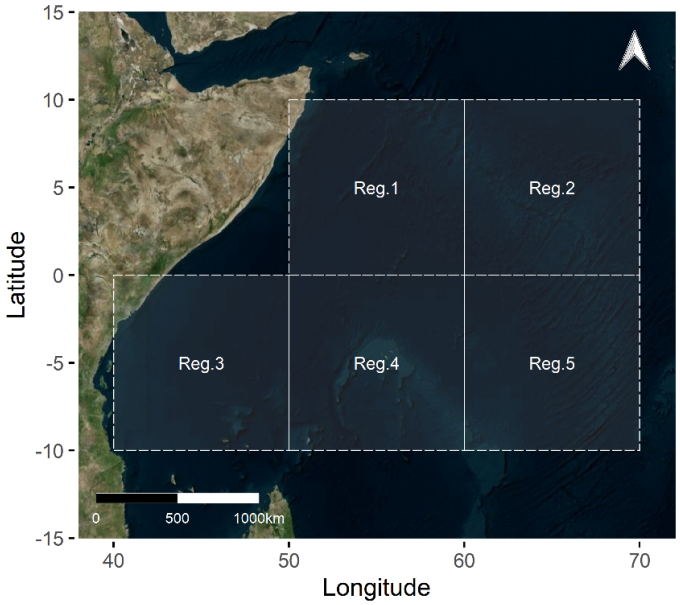

Figure 2: Spatial stratification of the study area

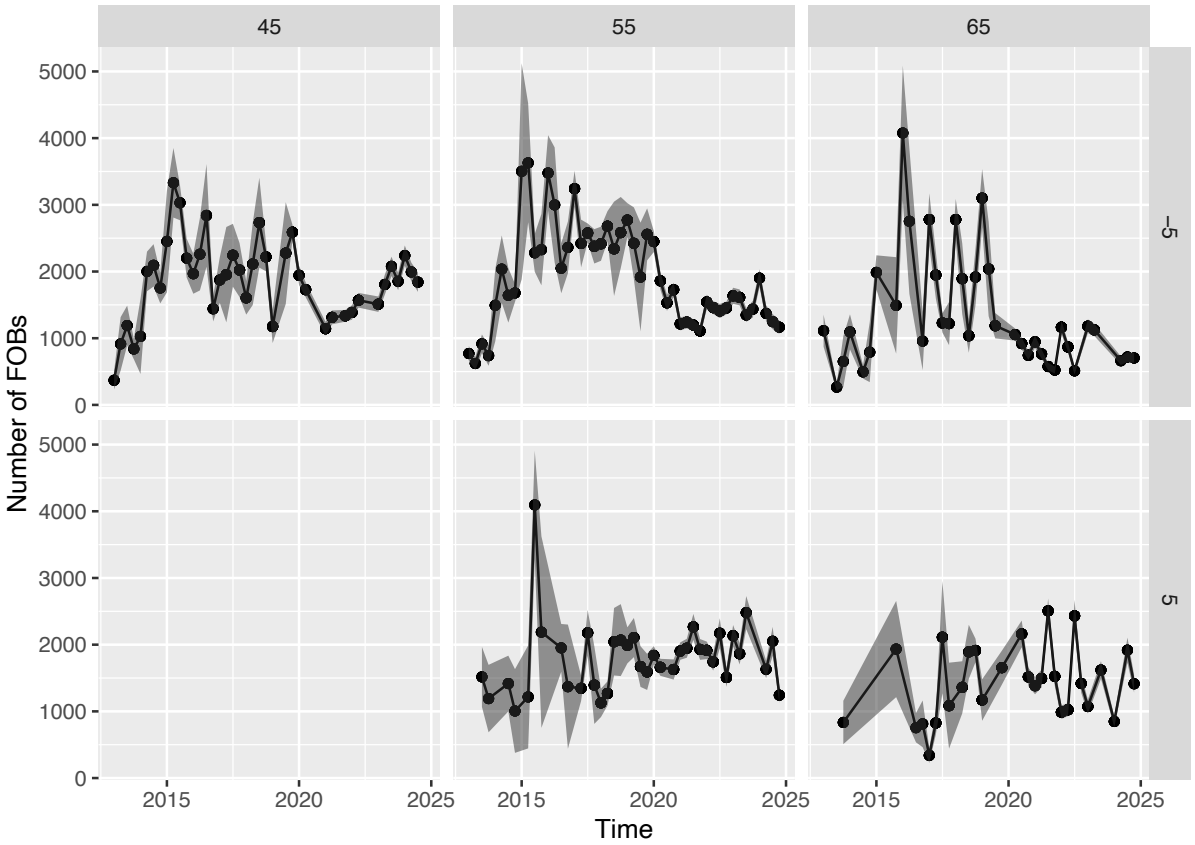

Figure 3: Quarterly estimates of the average number of floating objects in the study area (panels correspond to the study regions shown in Figure 2).

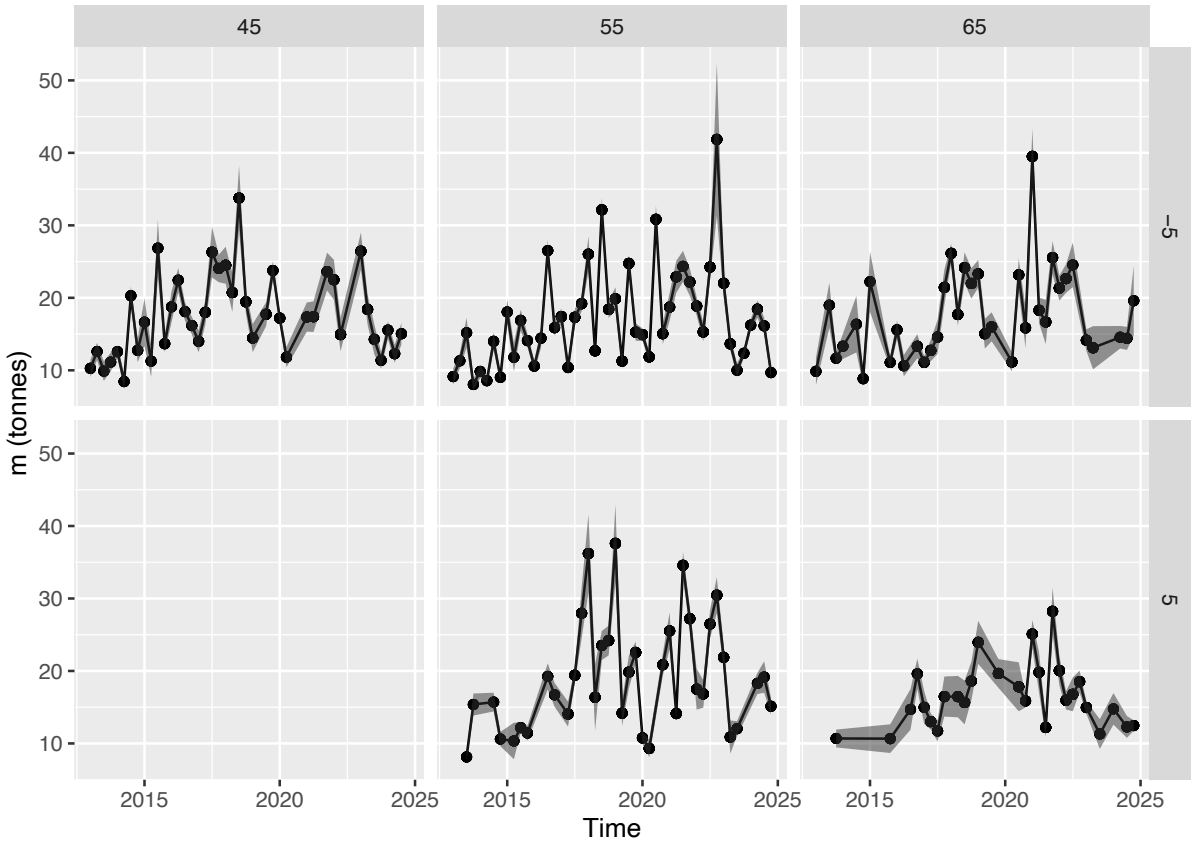

Figure 4: Quarterly estimates of the average biomass of skipjack tuna associated with a FOB ($\widehat{m}$) calculated for each stratum (panels correspond to the study regions shown in Figure 2).

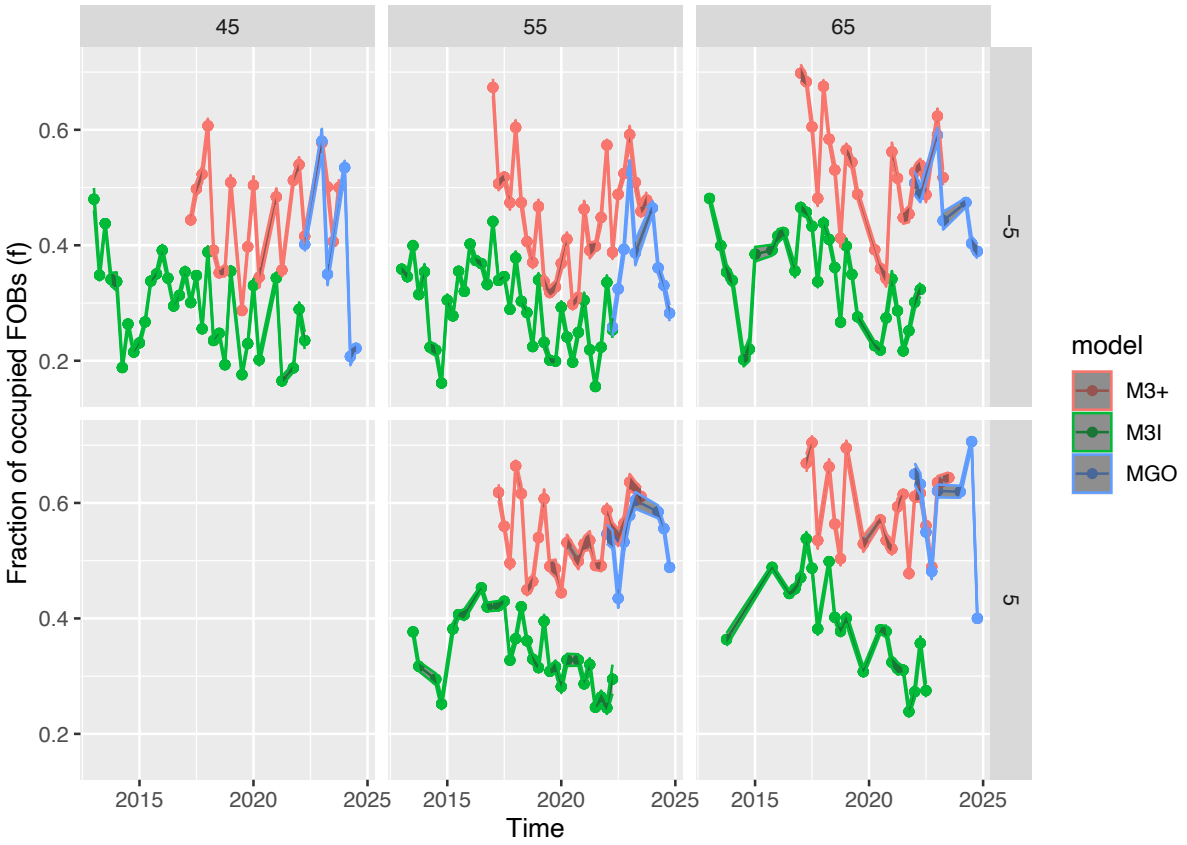

Figure 5: Quarterly estimates of the average proportion of FOBs occupied by skipjack tuna aggregations by 10°×10° spatial strata in the western Indian Ocean obtained for each buoy model (panels corresponds to the study regions shown in Figure 2).

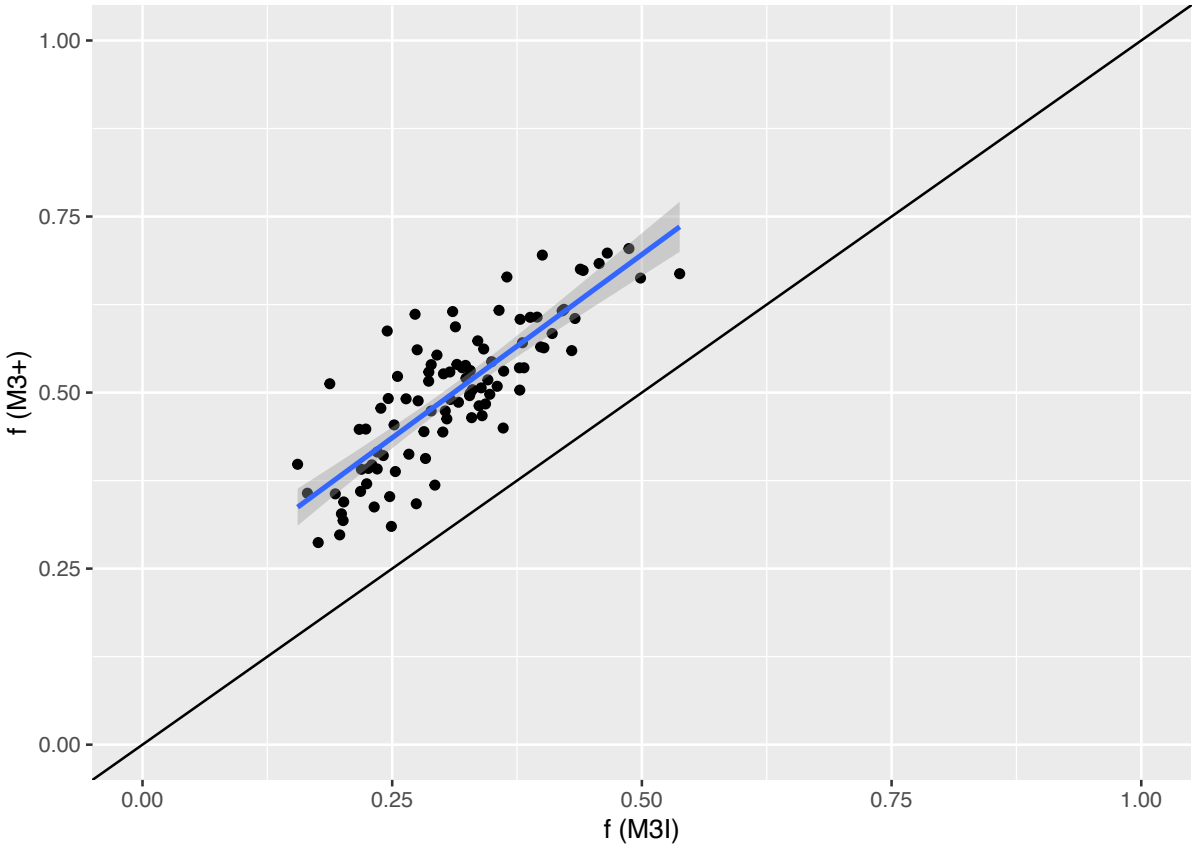

Figure 6: Correlation between the fraction of FOBs occupied by skipjack tuna aggregations obtained in the same spatio-temporal stratum using M3I and M3+ buoys. The black lines represents the y=x line and the blue line the fitted linear model.

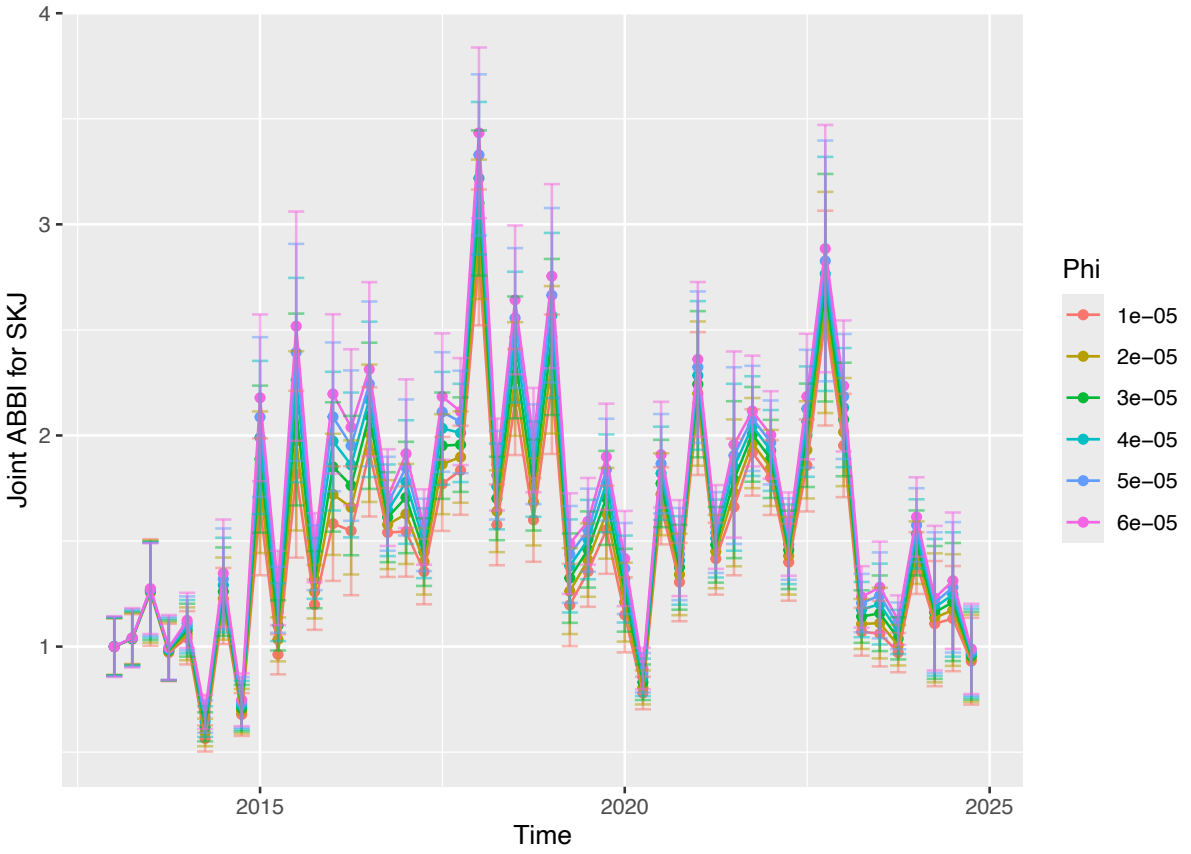

Figure 7: Relative joint ABBI index for skipjack tuna in the Western Indian ocean obtained by combining data from M3I, M3I+ and MGO buoy models. Colors indicate different value of the ϕ parameter (Eq.10).

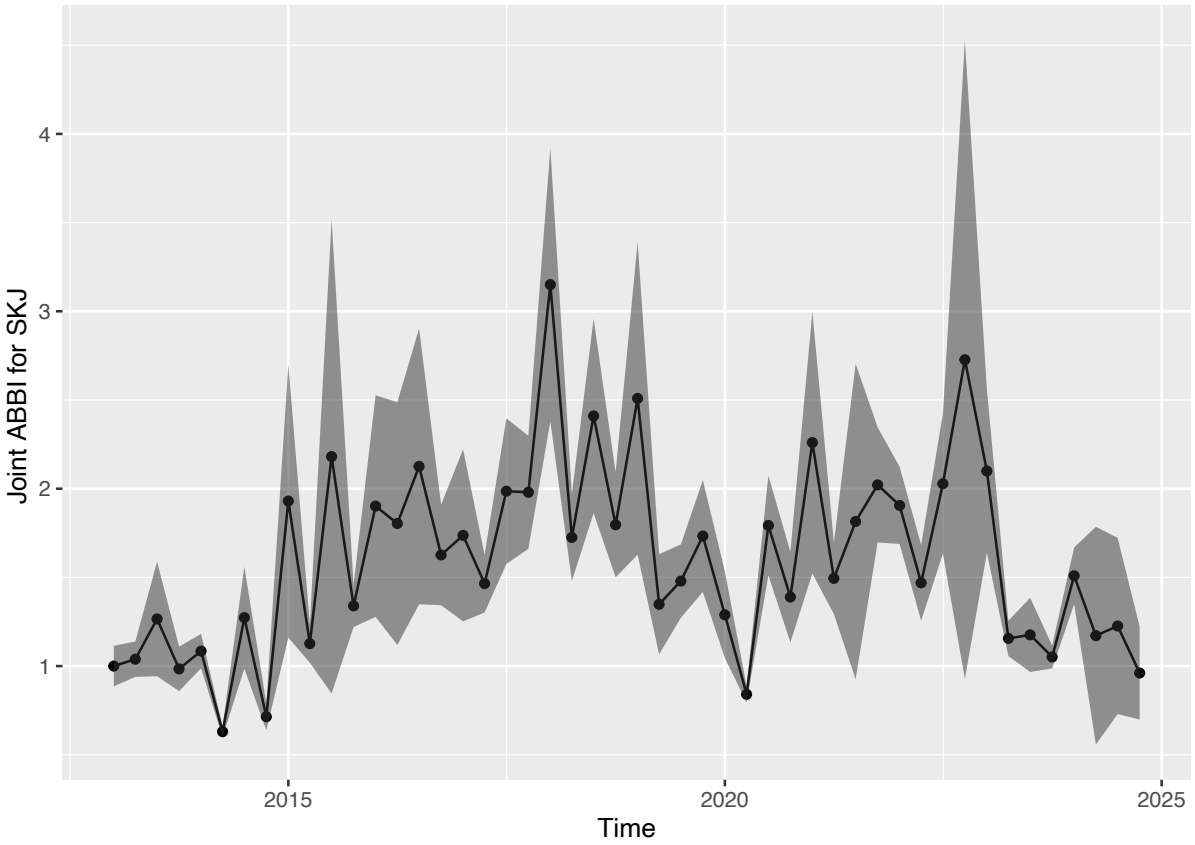

Figure 8: Relative joint ABBI index for skipjack tuna in the Western Indian ocean obtained by combining data from M3I and M3I+ buoy models and averaging over the ϕ parameter.

	Estimate	Std. Error	Pr(>|t|)
Intercept	0.17556	0.02417	1.09e-10
Slope	1.04097	0.07498	< 2e-16

Table 1: Results of the linear model fit used to explain the fraction of occupied FOBs estimated with M3I+ buoys as a function of the same estimates obtained with M3I buoys (Residual standard error: 0.05846 on 94 degrees of freedom; Multiple R-squared: 0.6722, Adjusted R-squared: 0.6687; F-statistic: 192.7 on 1 and 94 DF, p-value: < 2.2e-16).

ACKNOWLEDGEMENTS

The authors are grateful to ORTHONGEL and its contracting parties for providing the echosounder buoys data. The authors sincerely thank the contribution of the staff of the Ob7 on the databases of the echosounder buoys. We are also grateful to the buoy manufacturers for their useful advice and information on echosounder buoys.

REFERENCES

Bach, P., Cauquil, P., Depetris, M., Duparc, A., Floch, L., Lebranchu, J., and Sabarros, P. 2018. Procédures d'échantillonnage des thonidés tropicaux débarqués par les senneurs dans les océans Atlantique et Indien. ird-02132072. 70p pp. https://hal.ird.fr/ird-02132072.

Baidai, Y., Dagorn, L., Amande, M. J., Gaertner, D., and Capello, M. 2020. Machine learning for characterizing tropical tuna aggregations under Drifting Fish Aggregating Devices (DFADs) from commercial echosounder buoys data. Fisheries Research, 229: 105613. Elsevier. https://doi.org/10.1016/j.fishres.2020.105613.

Baidai, Y., Dupaix, A., Dagorn, L., Gaertner, D., Deneubourg, J.-L., Duparc, A., & Capello, M. (2024). Direct assessment of tropical tuna abundance from their associative behaviour around floating objects. Proceedings of the Royal Society B: Biological Sciences, 291(2029), 20241132.

Capello, M., Deneubourg, J. L., Robert, M., Holland, K. N., Schaefer, K. M., and Dagorn, L. 2016. Population assessment of tropical tuna based on their associative behavior around floating objects. Scientific Reports, 6: 36415. The Author(s). https://www.nature.com/articles/srep36415#supplementary-information.

Dagorn, L., Pincock, D., Girard, C., Holland, K., Taquet, M., Sancho, G., Itano, D., *et al.* 2007. Satellite-linked acoustic receivers to observe behavior of fish in remote areas. Aquatic Living Resources, 20: 307–312. http://www.alr-journal.org/10.1051/alr:2008001.

Depetris, M., and Lebranchu, J. 2020. OB7-IRD/t3: Beta version of T3 software (Version 0.9.0).

Diallo, A., Baidai, Y., Mannocci, L., & Capello, M. (2019). Towards the derivation of fisheries-independent abundance indices for tropical tuna: Report on biomass estimates obtained from a multi-frequency echosounder buoy model (M3I+). IOTC–2019–WPTT21–54. Working Party on Tropical Tunas (WPTT), Indian Ocean Tuna Commission (IOTC).

Dupaix, A., Capello, M., Lett, C., Andrello, M., Barrier, N., Viennois, G., and Dagorn, L. 2021. Surface habitat modification through industrial tuna fishery practices. ICES Journal of Marine Science, 78: 3075–3088. Oxford University Press. https://academic.oup.com/icesjms/article/78/9/3075/6368416.

Duparc, A., Cauquil, P., Depetris, M., Dewals, P., Floch, L., Gaertner, D., Hervé, A., *et al.* 2018. Assessment of accuracy in processing purse seine tropical tuna catches with the T3 methodology using French fleet data. Working Party on Tropical Tunas (WPTT), IOTC-2018-WPTT20-16 Assessment. 19p pp. https://www.iotc.org/sites/default/files/documents/2018/10/IOTC-2018-WPTT20-16_Rev1.pdf.

Goujon, M., Maufroy, A., Relot-Stirnemann, A., Moëc, E., Bach, P., Cauquil, P., and Sabarros, P. 2017. Collecting data on board French and Italian tropical tuna purse seiners with common observers: results of ORTHONGEL'S voluntary observer program OCUP (2013-2017) in the Indian ocean. IOTC-2017-WPDCS13-22_Rev1. 22 pp. https://www.iotc.org/sites/default/files/documents/2017/11/IOTC-2017-WPDCS13-22_Rev1_-_OBS_PS_FRA.pdf.

Govinden, R., Capello, M., Forget, F., Filmalter, J. D., and Dagorn, L. 2021. Behavior of skipjack (Katsuwonus pelamis), yellowfin (Thunnus albacares), and bigeye (T. obsesus) tunas associated with drifting fish aggregating devices (dFADs) in the Indian Ocean, assessed through acoustic telemetry. Fisheries Oceanography: fog.12536. https://onlinelibrary.wiley.com/doi/10.1111/fog.12536.

IOTC–SC28 2025. Report of the 28 th Session of the IOTC Scientific Committee. China, 1 – 5 December 2025. IOTC– 2025–SC28–R[E]: 269 pp.

IOTC–WPTT25 2023. Report of the 25 th Session of the IOTC Working Party on Tropical Tunas. San Sebastian, 30 October - 4 November 2023. IOTC–2023–WPTT25–R[E]: 94 pp.

Katara, I., Gaertner, D., Marsac, F., Grande, M., Kaplan, D., Agurtzane, U., Loreleï, G., *et al.* 2018. Standardisation of yellowfin tuna CPUE for the EU purse seine fleet operating in the Indian Ocean. 20th session of the Working Party on Tropical Tuna., IOTC–2018–WPTT20–36_Rev1. 1–14 pp. https://www.iotc.org/sites/default/files/documents/2018/10/IOTC-2018-WPTT20-36_Rev1.pdf.

Lenth, R. V. 2016. Least-Squares Means: The R Package lsmeans. Journal of Statistical Software, 69. http://www.jstatsoft.org/v69/i01/.

Matsumoto, T., Satoh, K., and Toyonaga, M. 2014. Behavior of skipjack tuna (Katsuwonus pelamis) associated with a drifting FAD monitored with ultrasonic transmitters in the equatorial central Pacific Ocean. Fisheries Research, 157: 78–85. Elsevier B.V. http://dx.doi.org/10.1016/j.fishres.2014.03.023.

Matsumoto, T., Satoh, K., Semba, Y., and Toyonaga, M. 2016. Comparison of the behavior of skipjack (Katsuwonus pelamis), yellowfin (Thunnus albacares) and bigeye (T. obesus) tuna associated with drifting FADs in the equatorial central Pacific Ocean. Fisheries Oceanography, 25: 565–581. http://doi.wiley.com/10.1111/fog.12173.

Ohta, I., and Kakuma, S. 2005. Periodic behavior and residence time of yellowfin and bigeye tuna associated with fish aggregating devices around Okinawa Islands, as identified with automated listening stations. Marine Biology, 146: 581–594. http://link.springer.com/10.1007/s00227-004-1456-x.

Pérez, G., Dagorn, L., Deneubourg, J. L., Forget, F., Filmalter, J. D., Holland, K., Itano, D., *et al.* 2020. Effects of habitat modifications on the movement behavior of animals: the case study of Fish Aggregating Devices (FADs) and tropical tunas. Movement Ecology, 8: 1–11. Movement Ecology.

Rigby, R., Stasinopoulos, M., Heller, G., and De Bastiani, F. 2019. Distributions for Modelling Location, Scale and Shape: Using GAMLSS in R. CRC Press. http://www.gamlss.com/wp-content/uploads/2018/01/DistributionsForModellingLocationScaleandShape.pdf.

Robert, M., Dagorn, L., Deneubourg, J. L., Itano, D., and Holland, K. 2012. Size-dependent behavior of tuna in an array of fish aggregating devices (FADs). Marine Biology, 159: 907–914.

Robert, M., Dagorn, L., Lopez, J., Moreno, G., and Deneubourg, J. L. 2013. Does social behavior influence the dynamics of aggregations formed by tropical tunas around floating objects? An experimental approach. Journal of Experimental Marine Biology

and Ecology, 440: 238–243.

Rodriguez-Tress, P., Capello, M., Forget, F., Soria, M., Beeharry, S., Dussooa, N., and Dagorn, L. 2017. Associative behavior of yellowfin Thunnus albacares, skipjack Katsuwonus pelamis, and bigeye tuna T. obesus at anchored fish aggregating devices (FADs) off the coast of Mauritius. Marine Ecology Progress Series, 570: 213–222. http://www.int-res.com/abstracts/meps/v570/p213-222/.

Tidd, A.N., Floc'h, L., Imzilen, T., Tolotti, M., Dagorn, L., Capello, M., & Guillotreau, P. (2023). How technical change has boosted fish aggregation device productivity in the Indian Ocean tuna fishery. Scientific Reports, 13, 17834.

Tolotti, M. T., Forget, F., Capello, M., Filmalter, J. D., Hutchinson, M., Itano, D., Holland, K., *et al.* 2020. Association dynamics of tuna and purse seine bycatch species with drifting fish aggregating devices (FADs) in the tropical eastern Atlantic Ocean. Fisheries Research, 226: 105521. Elsevier. https://doi.org/10.1016/j.fishres.2020.105521.